

STATUS OF THE MEIC ION COLLIDER RING DESIGN*

V.S. Morozov[#], Ya.S. Derbenev, L. Harwood, A. Hutton, F. Lin, F. Pilat, Y. Zhang,
 Jefferson Lab, Newport News, VA 23606, USA
 Y. Cai, Y.M. Nosochkov, M. Sullivan, M-H Wang, U. Wienands,
 SLAC, Menlo Park, CA 94025, USA
 J. Gerity, T. Mann, P. McIntyre, N.J. Pogue, A. Sattarov,
 Texas A&M University, College Station, TX 77843, USA

Abstract

We present an update on the design of the ion collider ring of the Medium-energy Electron-Ion Collider (MEIC) [1] proposed by Jefferson Lab. The design is based on the use of super-ferric magnets. It provides the necessary momentum range of 8 to 100 GeV/c for protons and ions, matches the electron collider ring design using PEP-II components, fits readily on the JLab site, offers a straightforward path for a future full-energy upgrade by replacing the magnets with higher-field ones in the same tunnel, and is more cost effective than using presently available current-dominated super-conducting magnets. We describe complete ion collider optics including an independently-designed modular detector region.

DESIGN OVERVIEW

The ion collider ring accelerates protons and ions from 8 to up to 100 GeV/c and is designed to provide luminosity above $10^{33} \text{ cm}^{-2}\text{s}^{-1}$ in the momentum range from 20 to 100 GeV/c. The overall layout of the ion collider ring indicating the main components is shown in Fig. 1. The ring consists of two 261.7° arcs connected by two straight sections intersecting at an 81.7° angle. The ion collider ring's geometry is determined by the electron collider ring [2,3]. The ion arcs are composed mainly of

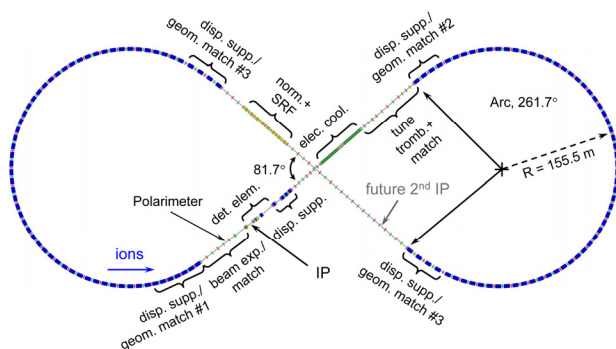


Figure 1: Layout and main components of the ion collider ring.

*Authored by Jefferson Science Associates, LLC under U.S. DOE Contracts No. DE-AC05-06OR23177 and DE-AC02-06CH11357. The U.S. Government retains a non-exclusive, paid-up, irrevocable, world-wide license to publish or reproduce this manuscript for U.S. Government purposes. Work supported in part by the US DOE Contract No. DE-AC02-76SF00515.

#morozov@jlab.org

FODO cells. The last few dipoles at either end of each arc are arranged to match the geometry of the ion collider ring. One of the straights houses an interaction region and is shaped to make a 50 mrad crossing angle with the electron beam at the interaction point. The second straight is mostly filled with FODO, however, retaining the capability of inserting a second interaction region. The overall ion ring circumference is 2153.89 m. The main building blocks of the ring are described below.

ARCS

The main building block of the ion arcs is a FODO cell shown in Fig. 2. It has been designed considering a balance of geometric, engineering and beam dynamical aspects. It has the same average bending radius as the electron arc. The ion FODO cell length is chosen at 22.8 m to be 1.5 times that of the electron FODO cell. Such a size allows for use of super-ferric magnets [4] up to a proton momentum of about 100 GeV/c. Each 8 m long dipole has a maximum field of about 3.06 T and bends the beam by about 4.2° with a bending radius of about 109.1 m.

The required magnet apertures are determined using a sum of a ± 10 rms beam size at injection (including betatron and dispersive contributions), a ± 1 cm closed orbit allowance, and, in case of dipoles, a plus or minus a half of the orbit arc's sagitta. To make the dipole horizontal aperture size more manageable, each dipole is implemented as two 4 m long straight pieces reducing the

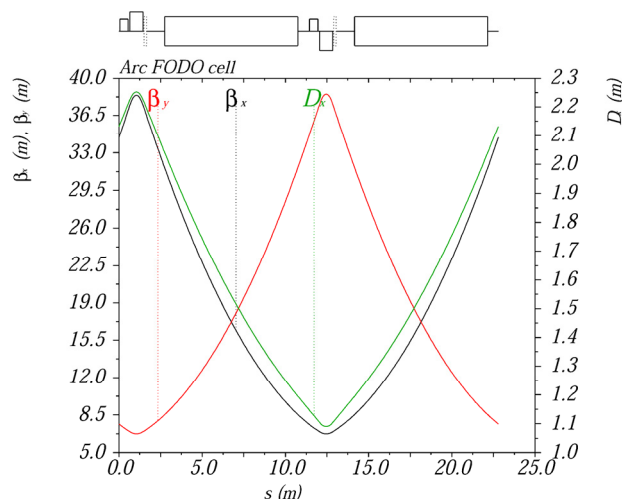


Figure 2: Ion arc FODO optics.

Content from this work may be used under the terms of the CC BY 3.0 licence (© 2015). Any distribution of this work must maintain attribution to the author(s), title of the work, publisher, and DOI.

sagitta to about 18 mm. The resulting required dipole good-field region is ± 5 and ± 3 cm in the horizontal and vertical planes, respectively. The required good-field region for all other magnets is circular with a radius of 4 cm. Sufficient space has been reserved in the lattice for magnet coil extensions: 14 cm at each end for dipoles and 5 cm at each end for most other magnets.

The maximum gradient of 0.8 m long FODO cell quadrupoles is about 53 T/m for a 90° betatron phase advance in both planes, which is straightforward to achieve with the super-ferric technology. We place a 0.5 m long corrector package on one side and a 15 cm long BPM on the other side of each quadrupole. Each corrector package includes horizontal and vertical orbit correctors, a skew quadrupole, and higher-order multipoles. The sextupoles in the corrector packages located in the dispersive regions are used for chromaticity compensation. With the above FODO cell parameters, the dispersive and betatron components of the beam size are comparable, which provides for an efficient use of the sextupole strength for chromaticity compensation. Nominally, each focusing sextupole of a FODO cell with a 3 T field at 4 cm radius adds 34.8/-7.1 units of horizontal/vertical chromaticity. Similarly, each defocusing sextupole adds -3.7/18.1 units of horizontal/vertical chromaticity per FODO cell. This leaves a sufficient margin for exploration of various chromaticity compensation schemes [5,6]. Two arc sextupole families could be used to generate horizontal and vertical chromatic beta waves to compensate the chromatic kicks of the final focusing quadrupoles. Two additional sextupole families could be used to compensate the residual chromaticities.

The bending angles and the spacing of the seven dipoles at the arc end upstream of the IP are adjusted to match the electron ring geometry and form a 50 mrad crossing angle at the IP as shown in Fig. 3a. The quadrupole strengths in this section are adjusted to suppress the dispersion while keeping the beta functions under control as shown in Fig. 3b. A four dipole section at the arc end downstream of the IP is adjusted to suppress the dispersion and provide a 1.5 m separation between the ion and electron beams. Similarly, four-dipole arc-end sections near the ends of the other straight are used to suppress the dispersion and match the electron ring shape.

INTERACTION REGION

The concept of the detector region design has been presented earlier [2,7]. Figure 4 shows the detector region optics. It starts at the end of one of the arcs and consists of a matching/ beam expansion section, upstream and downstream triplet Final Focusing Blocks (FFB), a spectrometer section, a geometric match/ dispersion suppression section, and a matching/ beam compression section. The matching sections contain a sufficient number of quadrupoles to control both the beta functions at the IP and the betatron phase advance for beta squeeze and chromaticity compensation. The upstream FFB is

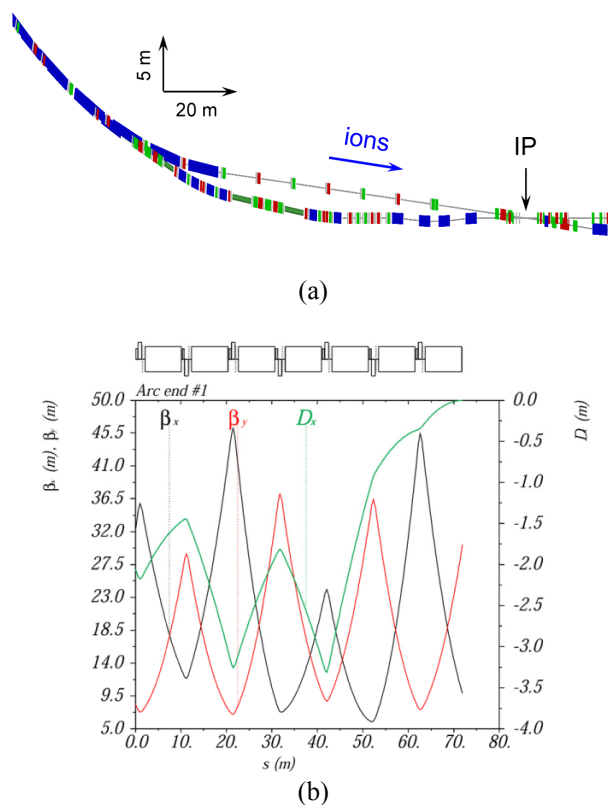


Figure 3: Geometry (a) and optics (b) of the arc end upstream of the IP.

closer to the IP than the downstream one to minimize their chromatic contribution while satisfying the detector requirements. The nominal horizontal and vertical beta function (beta-star) values at the IP are 10 and 2 cm, respectively. After the downstream FFB, there is an about 56 mrad spectrometer dipole followed by a machine-element-free 16 m space instrumented with detector elements. The subsequent four-dipole section suppresses the dispersion generated by the spectrometer dipole as well as adjusts the ion beam to be parallel to and

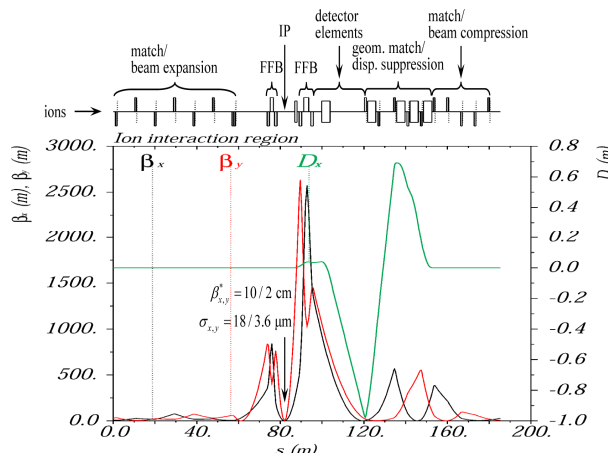


Figure 4: Ion interaction region optics.

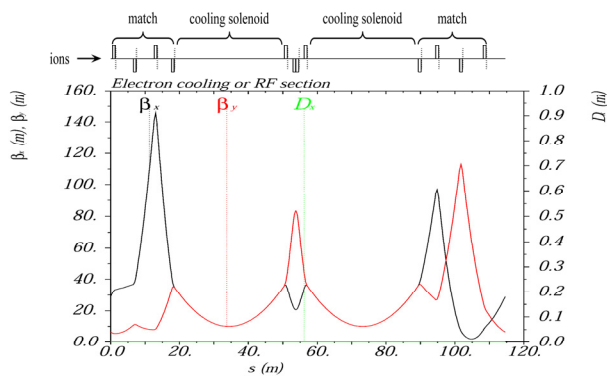


Figure 5: Electron cooling section.

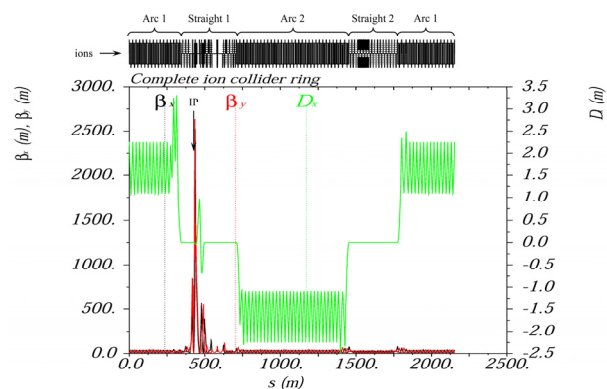


Figure 6: Complete ion collider ring optics.

separated by 1.5 m from the electron beam. This separation matches that at the arc end downstream of the IP formed by shaping the ion arc end as described above. Such a design makes the interaction region somewhat modular and decouples from the ring geometry providing for ease of integration into the ring lattice [2].

OTHER COMPONENTS

Another major component housed in the same straight as the interaction region is the electron cooling section [8] shown in Fig. 5. Two 30 m long drifts have been reserved for electron cooler solenoids. We plan to alternate the solenoid fields so that their net longitudinal field integral is zero to compensate their coupling and their effect on the ion spin. Optics based on triplet focusing is used to provide such long drifts. There is a matching segment at each end of the cooling section connecting it to the interaction region on one side and a straight FODO of a tune trombone on the other side.

The rest of the IP straight is occupied by a tune trombone for betatron tune adjustment. It consists of two FODO cells surrounded by matching sections. One of the matching sections is shared with the electron cooling section. The other matches FODO to the adjacent arc.

The second straight reserves space for a second IP and is presently filled with FODO lattice connected to arcs by

matching sections. Both accelerating and bunching RF cavities [9] are placed in this straight between the quadrupoles of the FODO lattice. The complete ion collider ring optics consisting of the components discussed above is shown in Fig. 6. Some of the ring's global parameters are summarized in Table 1. Note that crossing of the transition energy occurs during acceleration. However, existing experience shows that it can be handled efficiently using standard techniques [10]. A number of special elements has not been incorporated into the ring lattice at this stage but has been accounted for including injection kicker, beam abort system, electron cooler solenoids, spin control elements [11], polarimeter, crab cavities [12], and collimators.

Table 1: Some of the Parameters of the Ion Collider Ring

Parameter	Unit	Value
Momentum range	GeV/c	8-100
Circumference	m	2153.89
Arc bending angle	deg	261.7
Straights' crossing angle	deg	81.7
Maximum x/y β functions	m	2301/2450
Maximum x dispersion	m	3.28
x/y betatron tunes		24(.38)/24(.28)
x/y natural chromaticities		-101/-112
Momentum compaction		$6.45 \cdot 10^{-3}$
Transition γ		12.46
x/y norm. emittances	$\mu\text{m-rad}$	0.35/0.07
Maximum x/y beam size	mm	2.8/1.3

REFERENCES

- [1] F. Lin et al., these proceedings, TUYB3, Proc. of IPAC'15, Richmond, Virginia, USA (2015).
- [2] F. Lin et al., TUPAC28, Proc. of NA-PAC'13, Pasadena, California, USA (2013).
- [3] F. Lin et al., these proceedings, TUPTY084, Proc. of IPAC'15, Richmond, Virginia, USA (2015).
- [4] F.R. Huson et al., IEEE Trans. Nucl. Sci. **NS-32**, 3462 (1985).
- [5] V.S. Morozov et al., PRST-AB **16**, 011004 (2013).
- [6] Y.M. Nosochkov et al., these proceedings, TUPWI032, Proc. of IPAC'15, Richmond, Virginia, USA (2015).
- [7] V.S. Morozov et al., MOPRO005, Proc. of IPAC'14, Dresden, Germany (2014).
- [8] H. Zhang and Y. Zhang, TUPHO04, Proc. of NA-PAC'13, Pasadena, California, USA (2013).
- [9] S.Wang et al., WEPWO077, Proc. of IPAC'13, Shanghai, China (2013).

- Content from this work may be used under the terms of the CC BY 3.0 licence (© 2015). Any distribution of this work must maintain attribution to the author(s), title of the work, publisher, and DOI.
- [10] J. Kewisch and C. Montag, TPPB035, Proc. of PAC'03, Portland, Oregon, USA (2003).
[11] A.M. Kondratenko et al., MOPRO004, Proc. of IPAC'14, Dresden, Germany (2014).
[12] S. Ahmed et al., WEP082, Proc. of PAC'11, New York, USA (2011).